International Journal of Nanomedicine

Dovepress
open access to scientific and medical research

Open Access Full Text Article

ORIGINAL RESEARCH

Silver Nanotriangles and Chemotherapeutics Synergistically Induce Apoptosis in Glioma Cells via a ROS-Dependent Mitochondrial Pathway

This article was published in the following Dove Press journal:
International Journal of Nanomedicine

Huiquan Yang[1]
Wenbin Chen[1]
Jun Ma[2]
Jing Zhao[1]
Dongdong Li[1]
Yuyu Cao[1]
Peidang Liu[1,3]

[1]School of Medicine, Southeast University, Nanjing, Jiangsu, People's Republic of China; [2]Radiotherapy Department, Affiliated Hospital of Nanjing University of Chinese Medicine, Nanjing, Jiangsu, People's Republic of China; [3]Jiangsu Key Laboratory for Biomaterials and Devices, Southeast University, Nanjing, Jiangsu, People's Republic of China

Background: The synergistic effect of nanomaterials and chemotherapeutics provides a novel strategy for the treatment of tumors. Silver nanotriangles (AgNTs) exhibited some unique properties in nanomedicine. Studies on the synergy of silver-based nanomaterials and anti-tumor drugs against gliomas are rare.

Materials and Methods: Chitosan-coated AgNTs were prepared, followed by characterization using transmission electron microscopy, ultraviolet-visible spectroscopy and X-ray diffraction. The anti-glioma effect of cyclophosphamide (CTX), 5-fluorouracil (5-FU), oxaliplatin (OXA), doxorubicin (DOX) or gemcitabine (GEM) combined with AgNTs in different glioma cell lines (U87, U251 and C6) was assessed by the MTT assay to screen out a drug with the most broad-spectrum and strongest synergistic anti-glioma activity. The intracellular reactive oxygen species (ROS) level, mitochondrial membrane potential (MMP) and cell apoptosis were detected by flow cytometry. The possible underlying mechanisms of the synergy were further investigated with ROS scavenger and specific inhibitors of C-jun N-terminal kinase (JNK), p38 and extracellular signal-regulated kinase 1/2 pathways.

Results: The synthesized AgNTs were mainly triangular and truncated triangular with an average edge length of 125 nm. A synergistic anti-glioma effect of AgNTs combined with CTX was not observed, and the synergism between AgNTs and 5-FU was cell type-specific. AgNTs combined with OXA, DOX or GEM displayed synergistic effects in various glioma cell lines, and the combination of AgNTs and GEM showed the strongest synergistic activity. A decrease in cell viability, loss of the MMP and an increase in apoptosis rate induced by this synergy could be significantly attenuated by the ROS scavenger N-acetylcysteine and JNK inhibitor SP600125.

Conclusion: Our results suggested that the combination of AgNTs and GEM possessed broad-spectrum and potent synergistic anti-glioma activity, resulting from cell apoptosis mediated by a ROS-dependent mitochondrial pathway in which JNK might be involved.

Keywords: silver nanotriangles, chemotherapeutics, synergy, glioma

Introduction

Malignant gliomas are one of the most common and most serious types of intracranial tumors with high rates of recurrence and mortality.[1] The standard treatment for gliomas usually includes surgery, radiotherapy and chemotherapy. However, due to the extensive infiltration of glioma cells, complete resection is virtually impossible. Moreover, the effects of radiotherapy and chemotherapy are often limited by the resistance of highly malignant glioma cells.[2,3] Despite decades of efforts, the

Correspondence: Peidang Liu
School of Medicine, Southeast University, 87 Dingjiaqiao Road, Nanjing 210009, Jiangsu, People's Republic of China
Tel/Fax +86 25 8327 2554
Email seulpd@163.com

submit your manuscript | www.dovepress.com
DovePress
http://doi.org/10.2147/IJN.S267120

prognosis of glioma patients remains poor and the median overall survival time of glioblastoma patients after diagnosis is less than 15 months.[4] Thus, innovative methods are urgently needed to improve the treatment outcome.

Nanomaterials, with unique chemical, physical and optical properties, possess wide application potential in the current medical field. According to some previous reports, the combination of nanomaterials and chemotherapeutics could be a novel strategy to yield a greater therapeutic effect than that obtained by single-agent treatment. For example, the activity of cyclophosphamide against acute myeloid leukemia cells (CTX) was reported to be enhanced in the presence of silver nanoparticles (AgNPs).[5] Besides, 5-fluorouracil (5-FU) and AgNPs were observed to exhibit a synergistic anti-tumor effect in breast and lung cancer cells.[6] Similarly, the combination of oxaliplatin (OXA) and gold nanoparticles (AuNPs) displayed synergistic anti-tumor activity in human colonic adenocarcinoma cells.[7] It was also reported that doxorubicin (DOX) combined with AgNPs induced more apoptosis in breast cancer cells than AgNPs alone or DOX alone.[8] Moreover, AgNPs were confirmed to be able to enhance the pro-apoptotic ability of gemcitabine (GEM) in human ovarian cancer cells.[9] However, studies focused on the synergistic anti-tumor effects of metal nanomaterials and chemotherapy drugs in glioma cells are rare.

Because of their unusual anti-bacterial, anti-fungal, anti-viral and anti-cancer characteristics, silver-based nanomaterials have garnered considerable attention among various nanomaterials. Shapes play a crucial role in the properties of metal nanomaterials, and silver nanotriangles (AgNTs) were proved to have several obvious advantages over silver-based nanomaterials of other shapes. For instance, AgNTs possess superior antibacterial activity over spherical and rod-shaped AgNPs.[10] Apart from that, AgNTs with anisotropic shapes can be used as surface-enhanced Raman scattering nanotags for imaging of tumor cells.[11] Surface modification also affects the behavior of nanomaterials. The stability and biocompatibility of nanoparticles are improved if they are coated by the natural polymer chitosan.[12] Due to its special structure, chitosan can load chemotherapy drugs by diffusion and electrostatic interaction, which has been widely used in drug delivery system.[13] Furthermore, the chemical groups in chitosan can be conjugated with functional molecules for tumor-targeted diagnosis and therapy.[14,15]

According to the works mentioned above, CTX, 5-FU, OXA, DOX and GEM were separately reported to elicit anti-tumor synergy with AgNPs or AuNPs. Therefore, we were inspired to study the anti-tumor effects of these five drugs combined with chitosan-coated AgNTs in a variety of glioma cell lines and to investigate whether there was a drug with broad-spectrum and potent anti-glioma synergy when used in combination with AgNTs. Furthermore, the possible underlying mechanisms of such synergy were investigated. All findings obtained from our work might provide a theoretical basis for the development of highly efficacious therapy of gliomas.

Materials and Methods

Materials

Trisodium citrate, silver nitrate, sodium borohydride, chitosan, ascorbic acid, N-acetylcysteine (NAC), 3-(4,5-dimethylthiazol-2-yl)-2,5-diphenyltetrazolium bromide (MTT), reactive oxygen species (ROS) assay kit, JC-1 assay kit, and annexin V-fluorescein isothiocyanate (FITC)/propidium iodide (PI) apoptosis detection kit were ordered from Sigma–Aldrich (St. Louis, MO, USA). SP600125, SB203580 and U0126 were purchased from Abcam (Cambridge, UK). CTX, 5-FU, OXA, DOX and GEM were bought from Aladdin (Shanghai, China). U87, U251 and C6 glioma cell lines were obtained from the Type Culture Collection of the Chinese Academy of Sciences (Shanghai, China). All cell culture reagents were acquired from Gibco (Carlsbad, CA, USA).

Preparation of AgNTs

As described by Potara and colleagues, a seed-based growth method was applied to prepare AgNTs coated by chitosan, which served as a stabilizer and protective agent.[11] Briefly, 10 mL of trisodium citrate (2.5×10^{-4} M) and 10 mL of silver nitrate (2.9×10^{-4} M) were mixed and cooled in an ice-bath under vigorous stirring. To this mixture, 600 μL of sodium borohydride (0.1 M) was added dropwise, which resulted in a bright-yellow solution of seed particles. This seed solution was stored in darkness for 2–3 h at room temperature to allow excess sodium borohydride to react with water. Then, 10 mL of chitosan solution (2 mg/mL in 1% acetic acid), 50 μL of ascorbic acid (0.1 M), 400 μL of trisodium citrate (35 mM) and 200 μL of seed solution were mixed under continuous stirring at 35 ± 2°C, and 300 μL of silver nitrate (0.01 M) was subsequently dropped into the mixture within 1 min. The

growth of AgNTs was complete after approximately 5 min.

Characterization of AgNTs

The morphology of synthesized AgNTs was examined by transmission electron microscopy (TEM) using a JEM-2000EX system (Jeol, Tokyo, Japan). For TEM detection, the colloidal solution of AgNTs was dropped onto copper grids coated by carbon film and evaporated at room temperature for about 30 min. The edge length distribution was analyzed by measurement of 200 nanotriangles from random TEM images. The X-ray diffraction (XRD) pattern was collected by a D8 Discover X-ray diffractometer (Bruker, Karlsruhe, Germany) at a scan rate of 0.1 second per step at an operating voltage of 40 kV and current of 30 mA. An ultraviolet–visible (UV–vis) absorption spectrum was obtained using a UV-3600 spectrophotometer (Shimadzu, Tokyo, Japan). The zeta potential was determined by a Zetasizer Nano ZS (Malvern Instruments, Malvern, UK) through dynamic light scattering. The concentration of silver in the AgNTs solution was measured using inductively coupled plasma-mass spectrometry (PerkinElmer, Waltham, MA USA).

Cell Cultures

Cells were grown as a monolayer at 37°C in a humid atmosphere with 5% CO_2 in Dulbecco's modified Eagle's medium (DMEM) supplemented with 10% fetal bovine serum and 1% penicillin–streptomycin.

Measurement of Cell Viability

The MTT assay was conducted to determine the cell viability. In brief, 5×10^3 glioma cells per well were seeded in 96-well plates and cultured for 24 h before exposure to various concentrations of AgNTs, anti-tumor drugs (CTX, 5-FU, OXA, DOX or GEM) or their combinations. AgNTs and drugs were separately added into cell culture media for combination treatments. After 24 h of treatments, media were replaced by fresh media containing 0.5 mg/mL of MTT, followed by 4 h of incubation at 37°C in a cell incubator. After that, the formazan crystals formed were dissolved in dimethyl sulfoxide and a SpectraMax M5 microplate reader (Molecular Devices, Sunnyvale, CA, USA) was utilized to measure the absorbance at 570 nm. In each group, three independent biological repeats were performed.

Analysis of the Combined Effect

The combined effects of AgNTs and chemotherapeutics were assessed by the MTT assay. Cells were seeded in 96-well plates for 1 day before incubation with increasing concentrations of AgNTs alone or drugs alone (CTX, 5-FU, OXA, DOX or GEM) or with their combinations in various AgNTs-to-drug concentration ratios for 24 h. Then, a series of MTT assays were performed to determine the cell viability as described above. The Combination Index (CI) values were calculated using CompuSyn v1.0 (ComboSyn Inc., Paramus, NJ, USA) based on Chou and Talalay method.[16] CI values less than, equal to, and more than 1 indicated the effect of synergy, addition, and antagonism, respectively.

Measurement of Intracellular ROS

A ROS assay kit was applied to measure the intracellular ROS level after incubation with AgNTs, anti-tumor drug or their combination. Briefly, 1×10^5 U87 cells per well were seeded in 24-well plates and continuously cultured for 24 h. Then, after pretreatment with or without the ROS scavenger NAC (5 mM), fresh media containing AgNTs (4 μg/mL), GEM (0.1 μg/mL) or their combination were added, and incubation was conducted for another 24 h. Subsequently, cells were washed with phosphate-buffered saline (PBS), trypsinized, collected and loaded with 10 μM of the fluorescent probe 2′,7′-Dichlorodihydrofluorescein diacetate (DCFH-DA) in DMEM and incubation continued for 30 min in the dark at 37°C. A FACSCalibur flow cytometer (BD Biosciences, Franklin Lakes, NJ, USA) was used to measure the mean fluorescence intensity (MFI) with excitation at 488 nm and emission at 525 nm. For each sample, the intracellular ROS level was presented by determining the MFI of 10,000 cells.

Mitochondrial Membrane Potential (MMP) Measurement

The MMP was measured using the fluorescent probe JC-1. As a lipophilic cationic dye, JC-1 possesses a property of potential-dependent accumulation in mitochondria. In general, JC-1 dye enters mitochondria readily, accumulates, and emits red fluorescence. If the MMP decreases, the dye reagent will no longer aggregate in mitochondria and emit green fluorescence. In brief, U87 cells were pretreated with NAC (5 mM), the C-jun N-terminal kinase (JNK) inhibitor SP600125 (10 mM), the p38 inhibitor SB203580

(10 mM) or the extracellular signal-regulated kinase 1/2 (ERK1/2) inhibitor U0126 (10 mM) before treatment with AgNTs (4 μg/mL), GEM (0.1 μg/mL) or their combination for 24 h. Then, after 20 min of incubation with JC-1 at 37°C, cells were washed, harvested, resuspended in PBS, and flow cytometry was subsequently utilized to measure the fluorescence intensity of stained cells. The MMP was expressed as the ratio of red (aggregates) to green (monomers) fluorescence intensity.

Apoptosis Detection Assay

The annexin V-FITC/PI apoptosis detection kit was applied to investigate the cell apoptosis induced by AgNTs, GEM and their combination. Briefly, U87 cells were treated as mentioned above for 24 h. Then, cells were harvested and resuspended in 195 μL of binding buffer. To this buffer mixture, 5 μL of annexin V-FITC and 10 μL of PI were added consecutively, and the mixture was placed in darkness for 20 min at room temperature. Finally, cell apoptosis was analyzed using a flow cytometer.

Statistical Analysis

All data were obtained from at least three independent experiments and presented in the format of mean ± standard deviation (SD). SPSS v19.0 (IBM, Armonk, NY, USA) was applied to analyze differences between groups using one-way ANOVA with a post hoc test. A *P*-value of less than 0.05 was considered statistically significant.

Results and Discussion

Preparation and Characterization of AgNTs

Physical and chemical methods have been reported to be good choices for the controllable synthesis of metal nanoparticles.[17] In the current study, the method of AgNTs synthesis was a seed-based thermal synthetic procedure, which produced AgNTs in a rapid and reproducible manner.[18] As a commonly utilized nontoxic stabilizer and protective agent, chitosan was applied to stabilize the edges of the triangular particles and protect the particles against aggregation.[18] In addition, the biocompatibility of nanoparticles could be enhanced upon encapsulation by chitosan.[12]

The TEM characterization confirmed triangular and truncated triangular shapes of synthesized AgNTs (Figure 1A) and the average edge length was about 125 nm (Figure 1B). Two dipolar resonances at 783 nm (in-plane) and 400 nm (out-of-plane), and two quadrupolar resonances at 493 nm (in-plane) and 336 nm (out-of-plane) in the UV–vis absorption spectrum of the prepared solution (Figure 1C) were characteristics of AgNTs, according to a previous work.[12] Five distinct diffraction peaks was observed in the XRD pattern at 2θ values of 38.16°, 44.32°, 64.49°, 77.43° and 81.46°, which corresponded to the {111}, {200}, {220}, {311} and {222} planes of Ag (Figure 1D), revealing that the synthesized AgNTs had a face-centered-cubic crystal structure.[18] The zeta-potential of the prepared AgNTs was approximately 35 mV due to the existence of chitosan with positive ionic charge. Conjugation of AgNTs to chitosan was proved by Fourier transform infrared spectroscopy in our previous work.[21]

Combined Anti-Glioma Effects of AgNTs and Chemotherapeutics

In order to ascertain whether there was a drug with broad-spectrum and strong synergistic anti-glioma activity when combined with AgNTs, we detected the effects of AgNTs alone, drugs alone (CTX, 5-FU, OXA, DOX or GEM) and their combinations on the viability of three glioma cell lines (U87, U251 and C6) by the MTT assay. The inhibitory effects of AgNTs alone and anti-tumor drugs alone on the viability of glioma cells were observed to be dose-dependent (Figures 2–4). The CI values were calculated based on the concentrations and anti-glioma effects of AgNTs, drugs and their combinations to evaluate the combined effect (Table S1–3). In general, CI values more than, equal to and less than 1 mean antagonistic, additional and synergistic effects, respectively, and the smaller the CI value, the stronger the synergism.[22] The smallest CI values of the combined treatment of AgNTs plus different chemotherapeutics in the three cell lines and the corresponding concentration ratios were screened out from Table S1–3 and summarized in Table 1.

According to a previous work, the anti-tumor effect of CTX combined with AgNPs was synergistic in an acute myeloid leukemia cell line.[5] However, in the present study, a synergistic effect of CTX and AgNTs was not observed in glioma cells. The reason for this difference was possibly due to different cell lines or different shapes of silver nanomaterials. Besides, AgNTs displayed a synergistic effect with 5-FU only in C6 cell line but not in all cell lines tested, suggesting that the anti-glioma synergy between AgNTs and 5-FU might be cell type-specific.

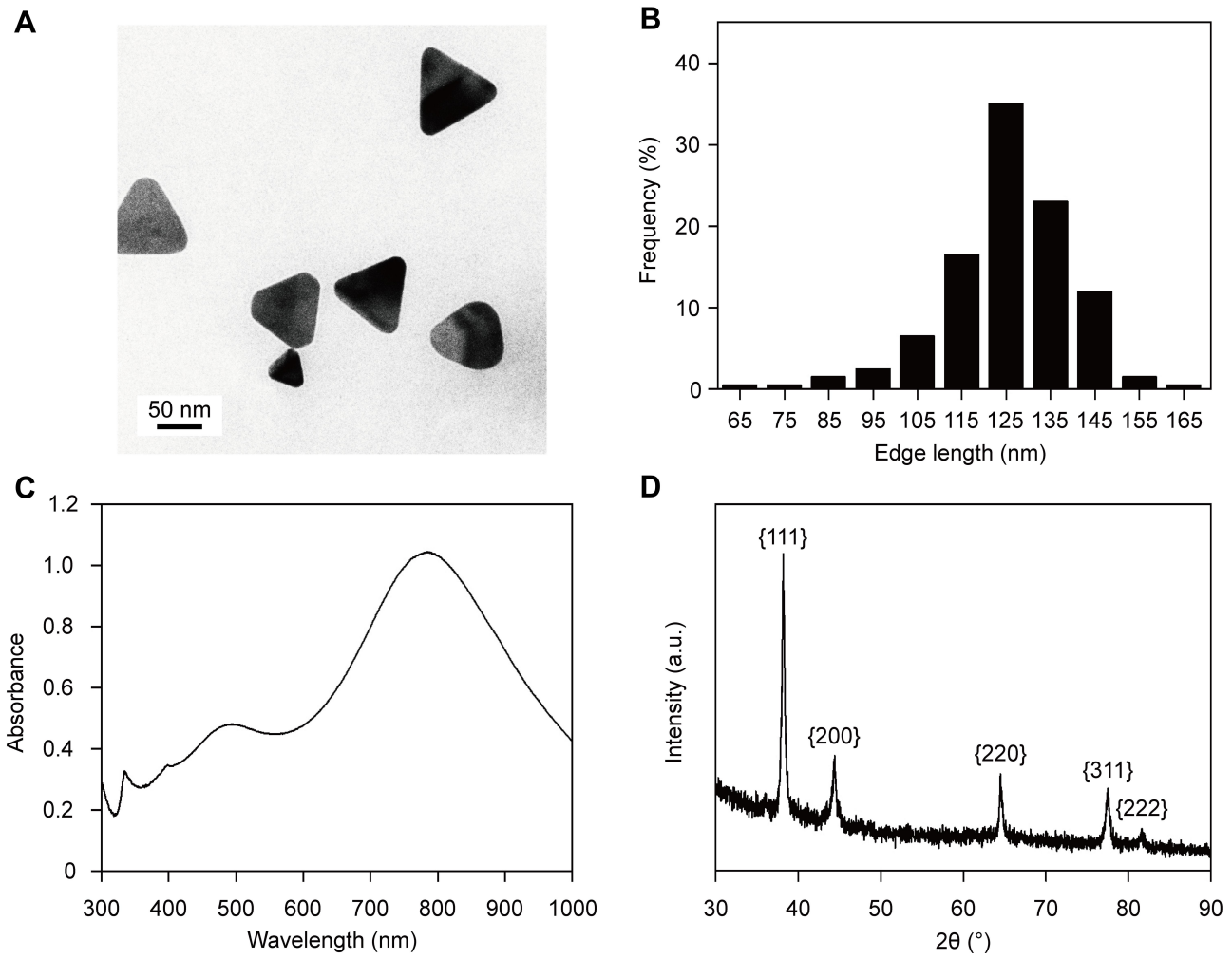

Figure 1 Characterization of AgNTs.
Notes: (**A**) TEM characterization and (**B**) edge length distribution histogram of AgNTs. The edge length distribution analysis was performed by measuring 200 nanotriangles. The mean edge length was about 125 nm. (**C**) UV–vis absorption spectrum and (**D**) XRD pattern of AgNTs.
Abbreviations: AgNTs, silver nanotriangles; TEM, transmission electron microscopy; UV–vis, ultraviolet–visible; XRD, X-ray diffraction.

The synergistic anti-tumor effect of OXA, DOX or GEM combined with AgNPs or AuNPs in colon, breast or ovarian cancer cells has been reported.[7,9,23] In the current study, these three drugs exerted broad-spectrum anti-glioma synergism with AgNTs, and the synergy between GEM and AgNTs was the strongest.

Chitosan on the surface of AgNTs enables loading chemotherapeutics by diffusion and electrostatic interaction.[13] According to the obtained optimal concentration ratio, drug-loaded silver nanocomposites with a synergistic anti-glioma effect can be prepared. The sustained release properties of chitosan can be applied to reduce the systemic toxicity of chemotherapy drug. Moreover, surface modification can promote the accumulation of nanocomposites in the brain and increase the ability to target glioma cells, thereby increasing the killing of tumor cells and reducing damage to normal tissues and organs.[24] The therapeutic effect and possible side effects of this strategy, as well as the elimination of AgNTs from the brain, need to be further studied in animal experiments.

Relationship Between ROS and the Anti-Tumor Synergy of AgNTs and GEM

Some literature reported that the production of ROS was a key mechanism of AgNPs toxicity,[25] and cell death induced by GEM was related to excess ROS production.[26] To investigate the relationship between ROS and the anti-glioma synergy of AgNTs and GEM, the effects of AgNTs, GEM or their combination on intracellular ROS levels in U87 cells were detected using the fluorescent probe, DCFH-DA. As shown in Figure 5A and

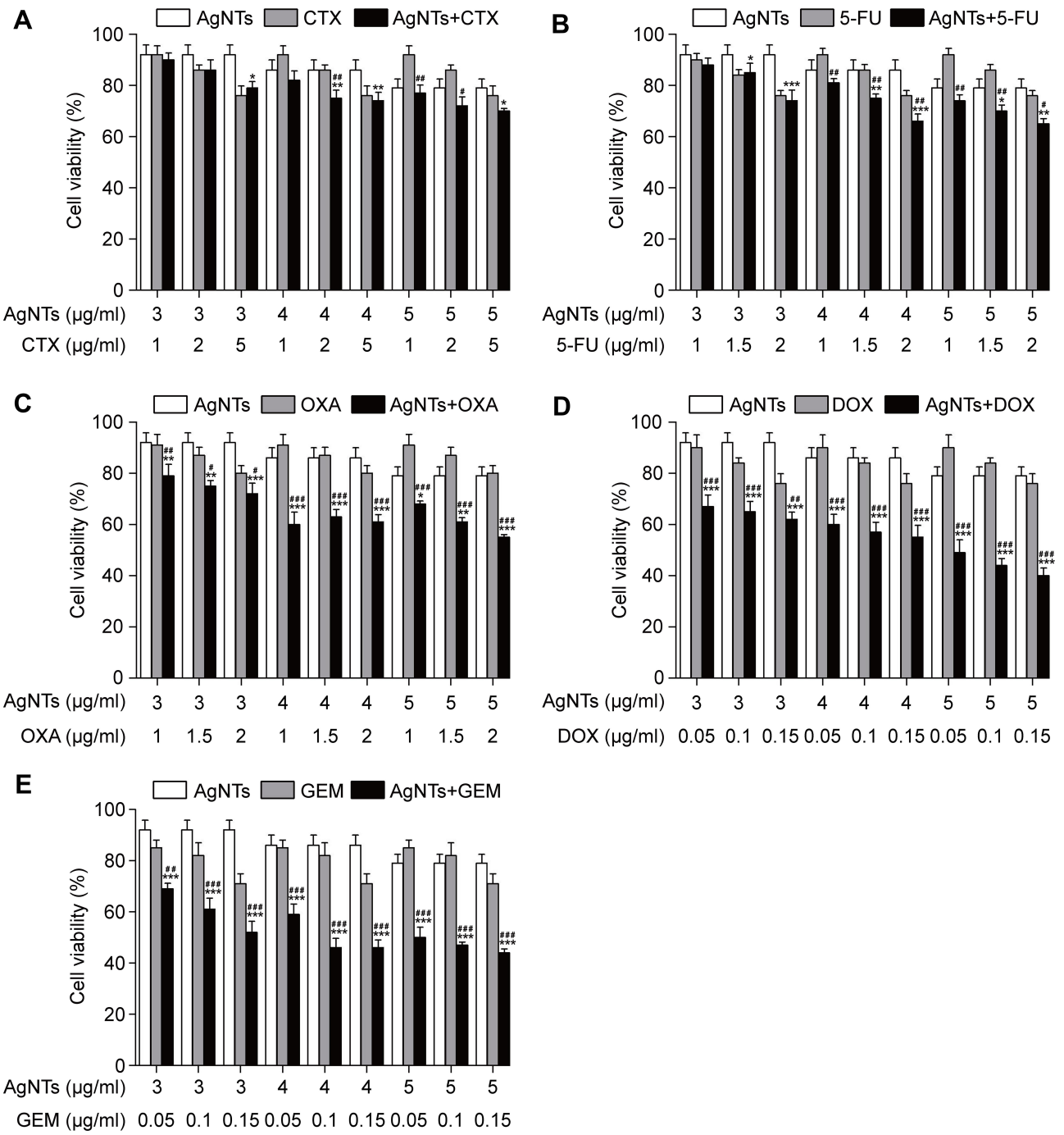

Figure 2 Effect of AgNTs, chemotherapeutics or their combinations on U87 cells viability.

Notes: The cell viability of U87 cells treated with various concentrations of AgNTs, CTX, 5-FU, OXA, DOX or GEM, or AgNTs plus one of these drugs in different AgNTs-to-drug concentration ratios for 24 h was evaluated by the MTT assay. The corresponding cell viability is shown in (**A**–**E**). Data are expressed as the mean ± SD determined from three independent experiments. When compared with the corresponding single AgNTs group, $^{*}P < 0.05$, $^{**}P < 0.01$, $^{***}P < 0.001$. When compared with the corresponding single drug group, $^{\#}P < 0.05$, $^{\#\#}P < 0.01$, $^{\#\#\#}P < 0.001$.

Abbreviations: AgNTs, silver nanotriangles; CTX, cyclophosphamide; 5-FU, 5-fluorouracil; OXA, oxaliplatin; DOX, doxorubicin; GEM, gemcitabine; MTT, 3-(4,5-dimethylthiazol-2-yl)-2,5-diphenyltetrazolium bromide; SD, standard deviation.

Figure S1, AgNTs, GEM and their combination treatment significantly increased ROS levels relative to control treatment, and the ROS level in the combination group was much higher than that in single-agent groups. Interestingly, the pretreatment with NAC was able to greatly reverse the increase of ROS levels induced by AgNTs, GEM and the combination. Further, the effect of ROS production on cell viability was evaluated by the MTT assay. The cell

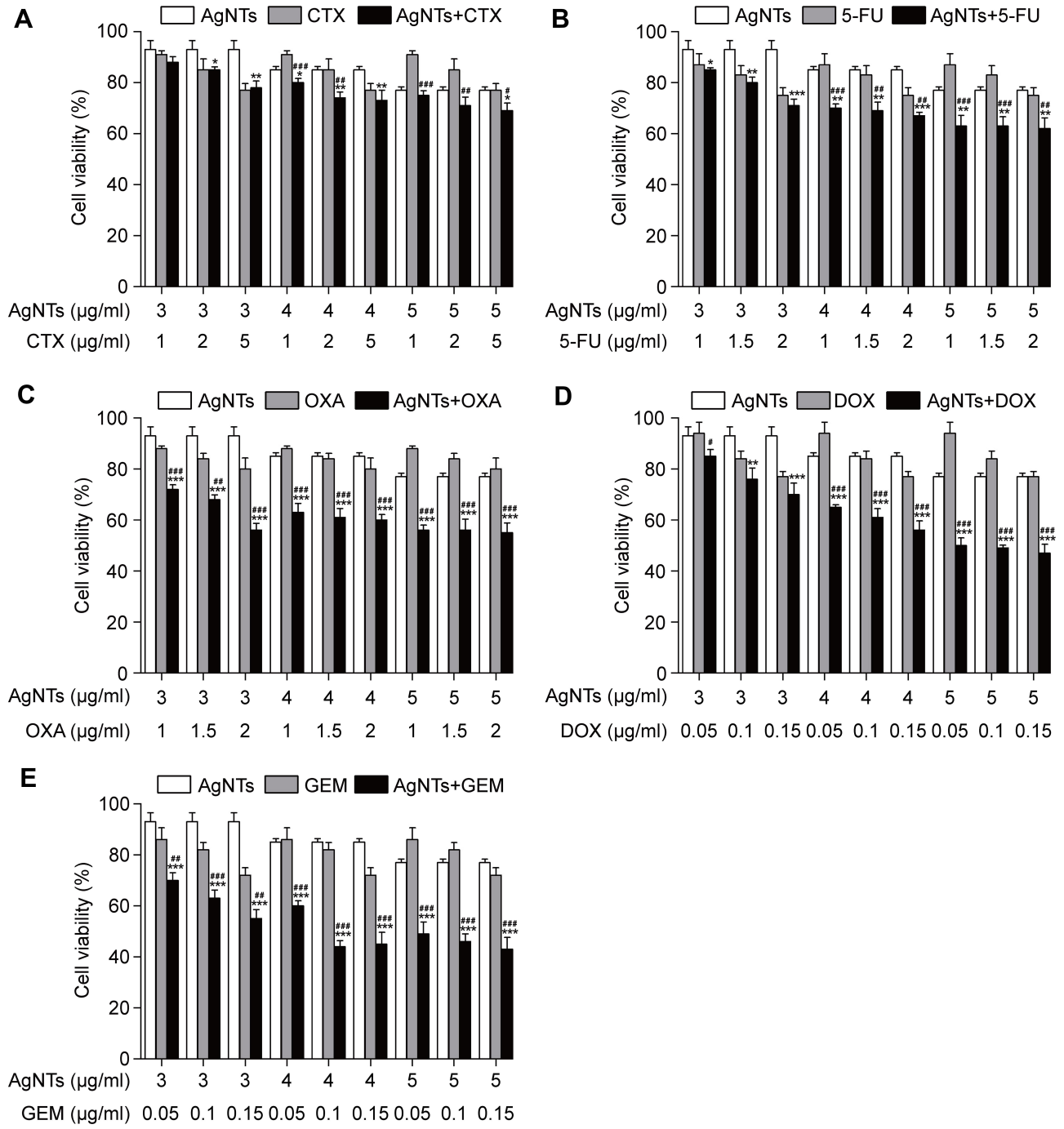

Figure 3 Effect of AgNTs, chemotherapeutics or their combinations on U251 cells viability.

Notes: The cell viability of U251 cells treated with various concentrations of AgNTs, CTX, 5-FU, OXA, DOX or GEM, or AgNTs plus one of these drugs in different AgNTs-to-drug concentration ratios for 24 h was assessed by the MTT assay. The corresponding cell viability is shown in (**A**–**E**). Data are shown as the mean ± SD summarized from three independent experiments. When compared with the corresponding single AgNTs group, $^{*}P < 0.05$, $^{**}P < 0.01$, $^{***}P < 0.001$. When compared with the corresponding single drug group, $^{\#}P < 0.05$, $^{\#\#}P < 0.01$, $^{\#\#\#}P < 0.001$.

Abbreviations: AgNTs, silver nanotriangles; CTX, cyclophosphamide; 5-FU, 5-fluorouracil; OXA, oxaliplatin; DOX, doxorubicin; GEM, gemcitabine; MTT, 3-(4,5-dimethylthiazol-2-yl)-2,5-diphenyltetrazolium bromide; SD, standard deviation.

viability decreased upon treatment with AgNTs, GEM and their combination, while the reduced cell viability could be significantly rescued by NAC pretreatment (Figure 5B), suggesting that the synergistic effect of AgNTs combined with GEM against glioma cells was closely related to ROS production.

As we all know, mitochondria are the major source of intracellular ROS. Overproduction of ROS is able to cause

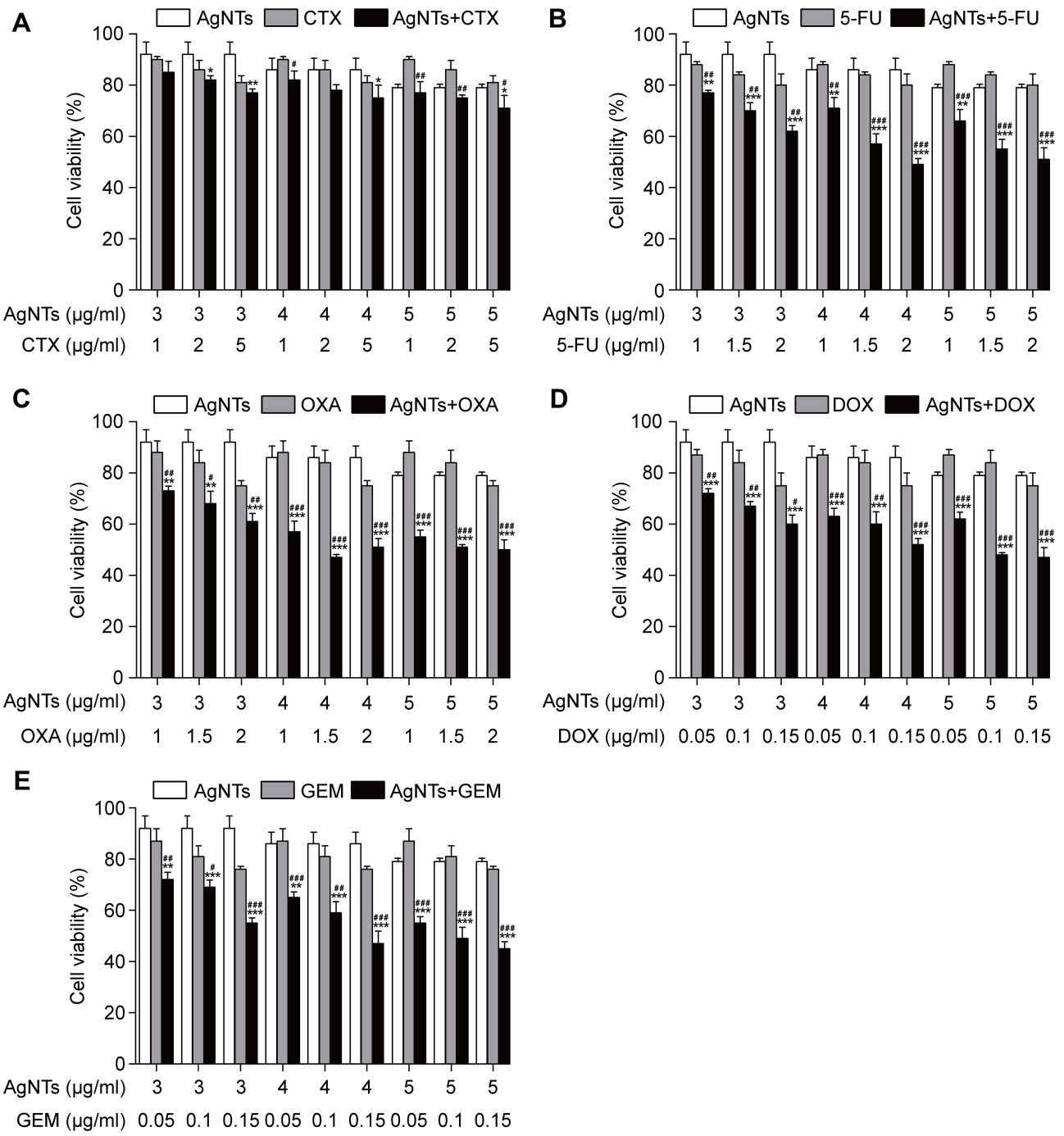

Figure 4 Effect of AgNTs, chemotherapeutics or their combinations on C6 cells viability.

Notes: The cell viability of C6 cells treated with various concentrations of AgNTs, CTX, 5-FU, OXA, DOX or GEM, or AgNTs plus one of these drugs in different AgNTs-to-drug concentration ratios for 24 h was determined by the MTT assay. The corresponding cell viability is shown in (**A**–**E**). Data are represented as the mean ± SD obtained from three independent experiments. When compared with the corresponding single AgNTs group, $^{*}P < 0.05$, $^{**}P < 0.01$, $^{***}P < 0.001$. When compared with the corresponding single drug group, $^{\#}P < 0.05$, $^{\#\#}P < 0.01$, $^{\#\#\#}P < 0.001$.

Abbreviations: AgNTs, silver nanotriangles; CTX, cyclophosphamide; 5-FU, 5-fluorouracil; OXA, oxaliplatin; DOX, doxorubicin; GEM, gemcitabine; MTT, 3-(4,5-dimethylthiazol-2-yl)-2,5-diphenyltetrazolium bromide; SD, standard deviation.

mitochondrial membrane dysfunction and dissipation of the MMP, ultimately leading to cell apoptosis.[27,28] Therefore, we next studied whether excess ROS production induced by single and combined treatments could result in MMP changes. U87 cells were incubated with AgNTs, GEM or their combination, after which the MMP was determined using the JC-1 assay. The results revealed that the MMP of cells exposed to AgNTs alone or GEM alone significantly decreased relative to that of

Table 1 Optimal Concentration Ratios of AgNTs and Chemotherapeutics and the Corresponding CI Values in the Combined Treatments of Glioma Cells

	U87			U251			C6		
	AgNTs (μg/mL)	Drugs (μg/mL)	CI	AgNTs (μg/mL)	Drugs (μg/mL)	CI	AgNTs (μg/mL)	Drugs (μg/mL)	CI
CTX	4	2	1.10	4	2	1.09	4	2	1.06
5-FU	4	2	1.30	5	1	1.08	4	2	0.62
OXA	4	1	0.75	3	2	0.65	4	1.5	0.68
DOX	5	0.1	0.60	5	0.05	0.79	5	0.1	0.63
GEM	4	0.1	0.53	4	0.1	0.59	4	0.15	0.56

Notes: The CI values were calculated based on the concentrations and anti-tumor effects of AgNTs, chemotherapeutics and their combinations in U87, U251 and C6 cells and summarized in supplementary material (Table S1–3). A CI value more than, equal to and less than 1 denote antagonistic, additional and synergistic effect, respectively. The smallest CI values and the corresponding concentration ratios were screened out from Table S1–3.

Abbreviations: AgNTs, silver nanotriangles; CI, combination index; CTX, cyclophosphamide; 5-FU, 5-fluorouracil; OXA, oxaliplatin; DOX, doxorubicin; GEM, gemcitabine.

untreated control cells, and the combined treatment resulted in a greater loss of the MMP than that observed upon single-agent treatments (Figure 6A). Besides, changes in the MMP could be reduced when cells were pretreated with NAC. Further, the apoptosis rate of U87 cells treated with AgNTs, GEM or their combination was detected by flow cytometry. AgNTs combined with GEM were able to induce remarkable cell apoptosis and the apoptosis percentage was much higher compared with that in single-agent groups (Figure 6B). Meanwhile, these pro-apoptotic effects of AgNTs, GEM and their combination were dramatically attenuated upon NAC pretreatment. These findings indicated that the combination of AgNTs and GEM could synergistically cause dissipation of the MMP and cell apoptosis, which were closely coupled with the overproduction of ROS. A previous study reported that AgNPs could decrease the MMP in U251 glioma cells and lead to cell apoptosis by enhancing ROS production.[29] A similar phenomenon induced by GEM was also observed in human ovarian cancer cells.[9] In the present study, AgNTs alone or GEM alone could reduce the MMP and promote cell apoptosis by inducing ROS production in U87 cells. Moreover, we found that the anti-glioma synergy between AgNTs and GEM was resulting from ROS-mediated mitochondrial dysfunction and cell apoptosis.

JNK, P38 and ERK1/2 Signaling Pathways and the Synergistic Anti-Glioma Effect of AgNTs and GEM

The mitogen-activated protein kinase (MAPK) signaling pathway exerts crucial functions in a variety of cellular

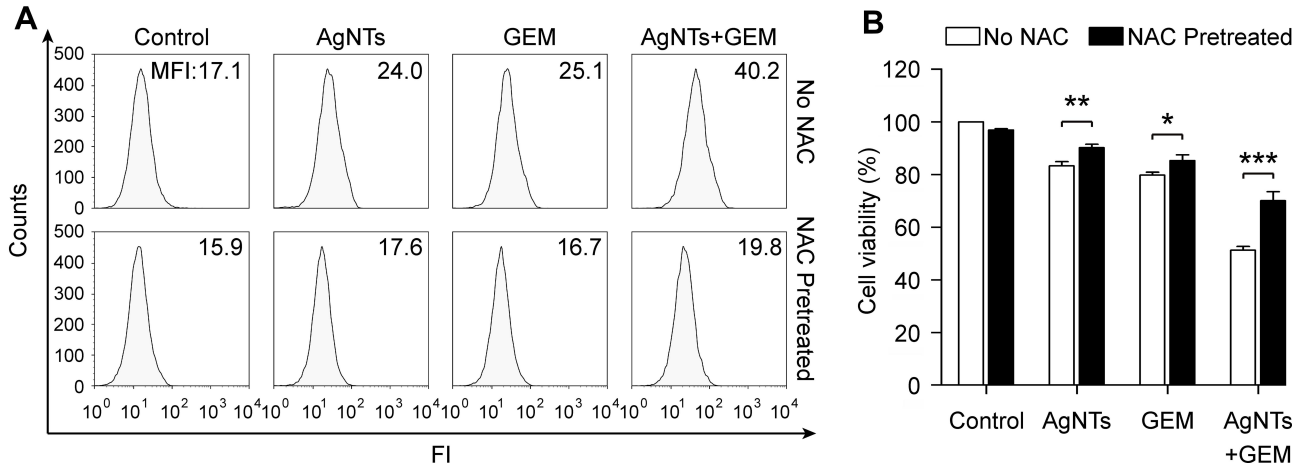

Figure 5 Effect of AgNTs, GEM or their combination on intracellular ROS production and viability of U87 cells pretreated with or without NAC.

Notes: U87 cells were exposed to AgNTs (4 μg/mL), GEM (0.1 μg/mL) or their combination for 24 h after pretreatment with or without NAC (5 mM). After that, cells were loaded with the ROS probe DCFH-DA and the MFI was quantified using flow cytometry. The cell viability was measured by the MTT assay. The intracellular ROS level and cell viability are shown in (**A**) and (**B**), respectively. The cell viability is expressed as the mean ± SD summarized from three independent experiments. When compared with the corresponding No NAC group, $^{*}P < 0.05$, $^{**}P < 0.01$, $^{***}P < 0.001$.

Abbreviations: AgNTs, silver nanotriangles; GEM, gemcitabine; ROS, reactive oxygen species; NAC, N-acetylcysteine; DCFH-DA, 2′,7′-dichlorofluorescein diacetate; MFI, mean fluorescence intensity; MTT, 3-(4,5-dimethylthiazol-2-yl)-2,5-diphenyltetrazolium bromide; SD, standard deviation.

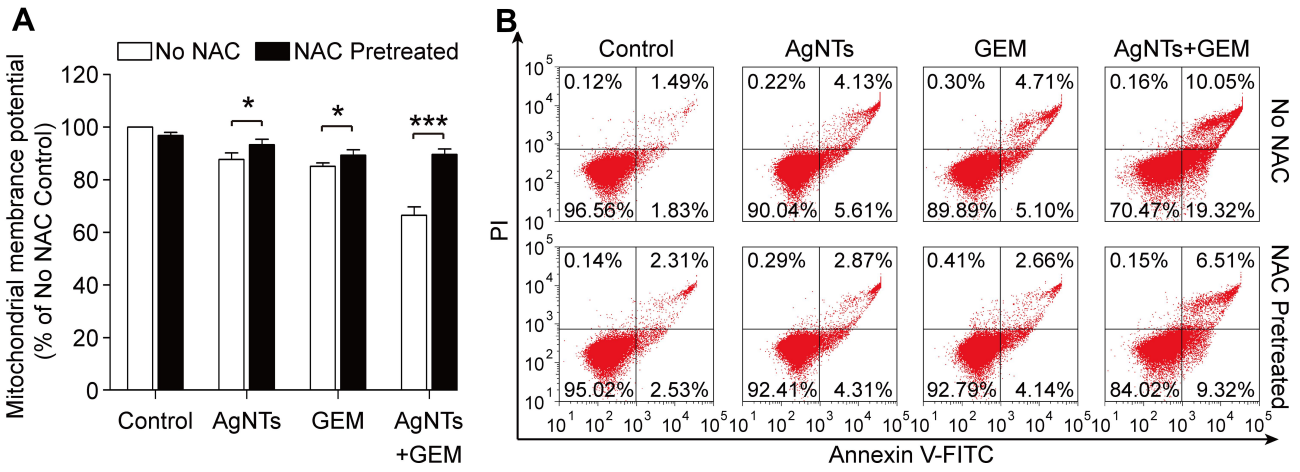

Figure 6 Effect of AgNTs, GEM or their combination on MMP and apoptosis of U87 cells pretreated with or without NAC.
Notes: After pretreatment with or without NAC (5 mM), U87 cells were incubated with AgNTs (4 μg/mL), GEM (0.1 μg/mL) or their combination for 24 h. (**A**) The MMP examined by the JC-1 assay. (**B**) Apoptosis rate determined by the annexin V-FITC/PI assay. The MMP is shown in the format of the mean ± SD obtained from three independent experiments. When compared with the corresponding No NAC group, $^{*}P < 0.05$, $^{***}P < 0.001$.
Abbreviations: AgNTs, silver nanotriangles; GEM, gemcitabine; MMP, mitochondrial membrane potential; NAC, N-acetylcysteine; FITC, fluorescein isothiocyanate; PI, propidium iodide; SD, standard deviation.

responses.[30,31] JNK, p38 and ERK1/2, important members of the MAPK family, have been proved to play vital roles in the formation, development and therapeutic response of tumors.[32–34] JNK and p38 MAPKs are generally associated with stress responses, cell differentiation and cell death.[35,36] Activation of ERK1/2 usually promotes cell survival, while ERK1/2 also has pro-apoptotic functions under certain conditions.[37] According to some previous works, these signaling pathways were involved in ROS-mediated cell apoptosis.[38–40]

In the present study, in order to elucidate the roles of JNK, p38 and ERK1/2 MAPK signaling pathways in the synergistic anti-glioma effect of AgNTs and GEM, we detected the effect of inhibition of these three pathways on the synergy by the MTT assay. For this purpose, U87 cells were pretreated with SP600125, SB203580 or U0126 before the treatment of AgNTs combined with GEM. As shown in Figure 7A, the reduction of cell viability was significantly rescued by SP600125, but not SB203580 or U0126. Next, the JC-1 assay and annexin V-FITC/PI apoptosis detection assay were, respectively, applied to further ascertain if the MMP and apoptosis level of cells treated with AgNTs plus GEM could be altered by these three inhibitors. We found that SP600125 could largely reduce the loss of the MMP induced by the combined treatment, whereas the effects of SB203580 and U0126 were not significant (Figure 7B). Similarly, the increased cell apoptosis rate caused by the combination was reversed only by SP600125 (Figure 7C). These results suggested the important role of the JNK signaling pathway in the synergistic anti-tumor effect of the combined treatment in glioma cells.

JNK, also known as stress-activated protein kinase, is responsive to many environmental stimuli, and plays pivotal roles in the cellular responses to environmental stress.[41] Studies have shown that JNK can be activated by ROS and serve as an important modulator in the process of ROS-induced cell death.[42,43] Active JNK is able to cause mitochondrial dysfunctions including loss of the MMP, permeability transition and release of cytochrome c, subsequently activating downstream pro-apoptotic caspases.[44] In the present study, overproduction of ROS, loss of the MMP and increased apoptosis rate were observed in U87 cells treated with the combined treatment of AgNTs and GEM. In addition, changes in the MMP and apoptosis level were reversed by NAC and SP600125, indicating that AgNTs combined with GEM could synergistically induce cell apoptosis via a ROS-dependent mitochondrial pathway and JNK might be involved in this process.

Conclusion

In the current study, the combined anti-glioma effects of AgNTs with five anti-tumor drugs (CTX, 5-FU, OXA, DOX and GEM) were evaluated. A synergistic effect of AgNTs combined with CTX was not observed, while the synergism of AgNTs and 5-FU was found to be cell type-specific. Besides, AgNTs combined with OXA, DOX or

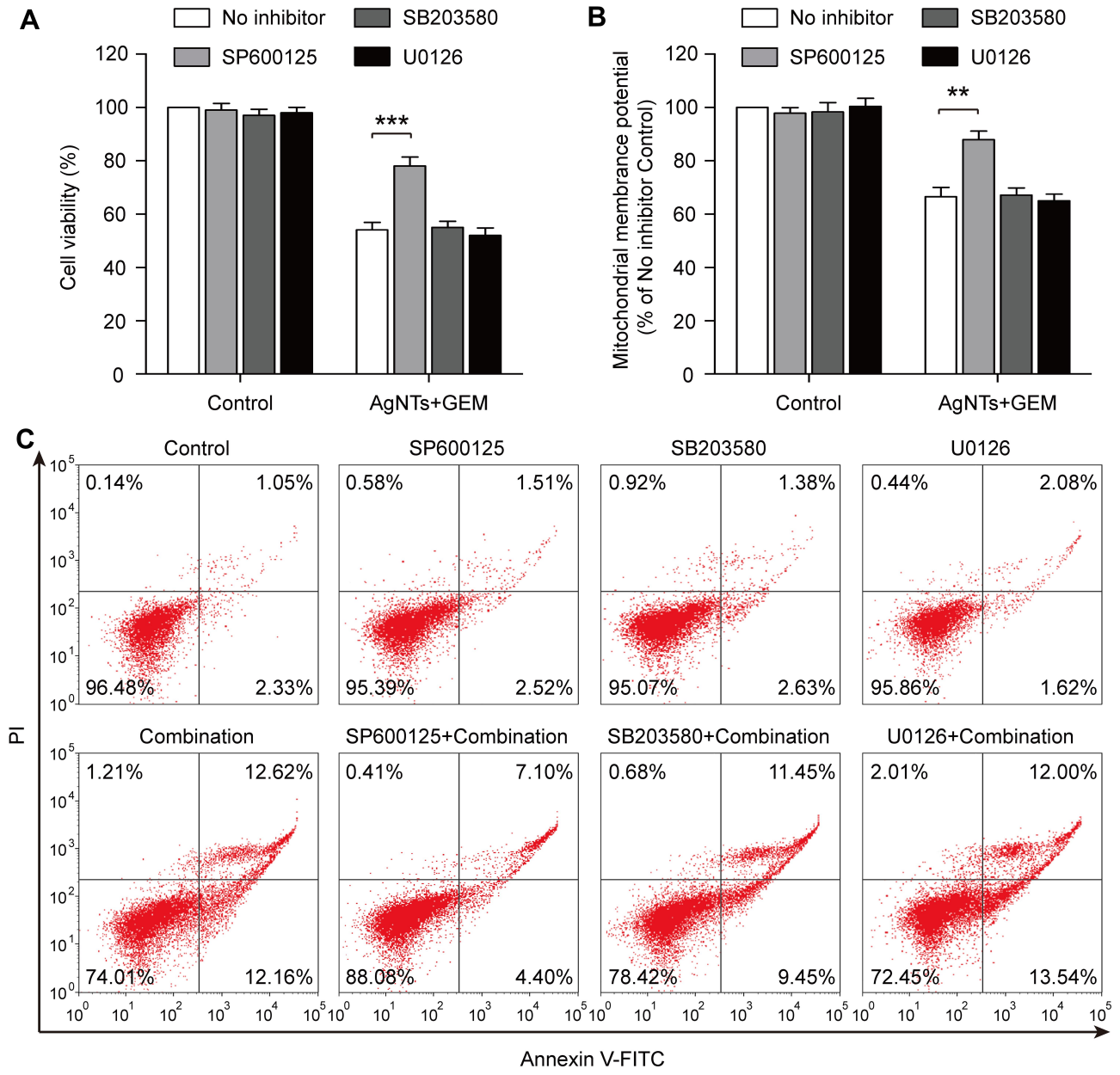

Figure 7 Effect of combined treatment of AgNTs and GEM on cell viability, MMP and cell apoptosis in the presence or absence of inhibitors of JNK, p38 and ERK1/2 MAPK signaling pathways.

Notes: U87 cells were pretreated with or without SP600125 (10 mM), SB203580 (10 mM) or U0126 (10 mM) before treatment with AgNTs (4 μg/mL), GEM (0.1 μg/mL) or their combination for 24 h. (**A**) The cell viability evaluated by the MTT assay. (**B**) The MMP detected by the JC-1 assay. (**C**) Apoptosis rate assessed by the annexin V-FITC/PI assay. The cell viability and MMP are represented as the mean ± SD obtained from three independent experiments. When compared with the corresponding No NAC group, $^{**}P < 0.01$, $^{***}P < 0.001$.

Abbreviations: AgNTs, silver nanotriangles; GEM, gemcitabine; MMP, mitochondrial membrane potential; MAPK, mitogen-activated protein kinase; MTT, 3-(4,5-dimethylthiazol-2-yl)-2,5-diphenyltetrazolium bromide; FITC, fluorescein isothiocyanate; PI, propidium iodide; SD, standard deviation.

GEM exhibited a synergistic anti-tumor effect in all glioma cell lines tested, and the synergy between AgNTs and GEM was the strongest. Moreover, this synergistic effect was found to be closely related to cell apoptosis mediated through a ROS-dependent mitochondrial pathway, in which JNK might play a vital part. Our findings might be exploited for new efficient combination strategies in glioma therapy.

Funding

This work was supported by the National Natural Science Foundation of China (81771980, 81571805 and

81703758), and the National Key Basic Research Program of China (973 Program; 2013CB933904).

Disclosure

The authors report no conflicts of interest in this work.

References

1. Wang J, Hu G, Quan X. Analysis of the factors affecting the prognosis of glioma patients. *Open Med*. 2019;14:331–335. doi:10.1515/med-2019-0031
2. Wang C, Zheng W, Yao D, et al. Upregulation of DNA metabolism-related genes contributes to radioresistance of glioblastoma. *Hum Gene Ther Clin Dev*. 2019;30(2):74–87. doi:10.1089/humc.2018.251
3. Zeng F, Wang K, Liu X, Zhao Z. Comprehensive profiling identifies a novel signature with robust predictive value and reveals the potential drug resistance mechanism in glioma. *Cell Commun Signal*. 2020;18(1):2. doi:10.1186/s12964-019-0492-6.
4. Frosina G. Limited advances in therapy of glioblastoma trigger re-consideration of research policy. *Crit Rev Oncol Hematol*. 2015;96(2):257–261. doi:10.1016/j.critrevonc.2015.05.013
5. Thombre RS, Mehta S, Mohite J, Jaisinghani P. Synthesis of silver nanoparticles and its cytotoxic effect against THP-1 cancer cell line. *Int J Pharma Bio Sci*. 2013;4:184–192.
6. Matai I, Sachdev A, Gopinath P. Multicomponent 5-fluorouracil loaded PAMAM stabilized-silver nanocomposites synergistically induce apoptosis in human cancer cells. *Biomater Sci*. 2015;3(3):457–468. doi:10.1039/c4bm00360h
7. Tummala S, Kumar MNS, Pindiprolu SK. Improved anti-tumor activity of oxaliplatin by encapsulating in anti-DR5 targeted gold nanoparticles. *Drug Deliv*. 2016;23(9):3505–3519. doi:10.1080/10717544.2016.1199606
8. Hekmat A, Saboury AA, Divsalar A. The effects of silver nanoparticles and doxorubicin combination on DNA structure and its antiproliferative effect against T47D and MCF7 cell lines. *J Biomed Nanotechnol*. 2012;8(6):968–982. doi:10.1166/jbn.2012.1451
9. Yuan Y, Peng Q, Gurunathan S. Silver nanoparticles enhance the apoptotic potential of gemcitabine in human ovarian cancer cells: combination therapy for effective cancer treatment. *Int J Nanomedicine*. 2017;12:6487–6502. doi:10.2147/IJN.S135482
10. Pal S, Tak YK, Song JM. Does the antibacterial activity of silver nanoparticles depend on the shape of the nanoparticle? A study of the Gram-negative bacterium Escherichia coli. *Appl Environ Microbiol*. 2007;73(6):1712–1720. doi:10.1128/AEM.02218-06
11. Potara M, Boca S, Licarete E, et al. Chitosan-coated triangular silver nanoparticles as a novel class of biocompatible, highly sensitive plasmonic platforms for intracellular SERS sensing and imaging. *Nanoscale*. 2013;5(13):6013–6022. doi:10.1039/c3nr00005b
12. Frank LA, Onzi GR, Morawski AS, Pohlmann AR, Guterres SS, Contri RV. Chitosan as a coating material for nanoparticles intended for biomedical applications. *React Funct Polym*. 2019;147:104459. doi:10.1016/j.reactfunctpolym.2019.104459
13. Li J, Cai C, Li J, et al. Chitosan-based nanomaterials for drug delivery. *Molecules*. 2018;23(10):2661. doi:10.3390/molecules23102661
14. Jun SW, Manivasagan P, Kwon J, et al. Folic acid-conjugated chitosan-functionalized graphene oxide for highly efficient photoacoustic imaging-guided tumor-targeted photothermal therapy. *Int J Biol Macromol*. 2020;155:961–971. doi:10.1016/j.ijbiomac.2019.11.055
15. Liu S, Li W, Gai S, et al. A smart tumor microenvironment responsive nanoplatform based on upconversion nanoparticles for efficient multimodal imaging guided therapy. *Biomater Sci*. 2019;7(3):951–962. doi:10.1039/c8bm01243a
16. Chou TC. Drug combination studies and their synergy quantification using the Chou-Talalay method. *Cancer Res*. 2010;70(2):440–446. doi:10.1158/0008-5472.CAN-09-1947
17. Huang Z, Jiang X, Guo D, Gu N. Controllable synthesis and biomedical applications of silver nanomaterials. *J Nanosci Nanotechnol*. 2011;11(11):9395–9408. doi:10.1166/jnn.2011.5317
18. Aherne D, Ledwith DM, Gara M, Kelly JM. Optical properties and growth aspects of silver nanoprisms produced by a highly reproducible and rapid synthesis at room temperature. *Adv Funct Mater*. 2008;18(14):2005–2016. doi:10.1002/adfm.200800233
19. Thompson EA, Graham E, MacNeill CM, et al. Differential response of MCF7, MDA-MB-231, and MCF 10A cells to hyperthermia, silver nanoparticles and silver nanoparticle-induced photothermal therapy. *Int J Hyperthermia*. 2014;30(5):312–323. doi:10.3109/02656736.2014.936051
20. Potara M, Gabudean AM, Astilean S. Solution-phase, dual LSPR-SERS plasmonic sensors of high sensitivity and stability based on chitosan-coated anisotropic silver nanoparticles. *J Mater Chem*. 2011;21(11):3625–3633. doi:10.1039/c0jm03329d
21. Liu P, Yang H, Chen W, Zhao J, Li D. Silver nanotriangles and chemotherapy drugs synergistically induce apoptosis in breast cancer cells via production of reactive oxygen species. *J Nanopart Res*. 2019;21(11):250. doi:10.1007/s11051-019-4703-2
22. Xu W, Ma W, Zeng H. Synergistic effect of ethaselen and selenite treatment against A549 human non-small cell lung cancer cells. *Asian Pac J Cancer Prev*. 2014;15(17):7129–7135. doi:10.7314/apjcp.2014.15.17.7129
23. Wang F, Wang Y, Dou S, et al. Doxorubicin-tethered responsive gold nanoparticles facilitate intracellular drug delivery for overcoming multidrug resistance in cancer cells. *ACS Nano*. 2011;5(5):3679–3692. doi:10.1021/nn200007z
24. Saraiva C, Praça C, Ferreira R, et al. Nanoparticle-mediated brain drug delivery: overcoming blood-brain barrier to treat neurodegenerative diseases. *J Control Release*. 2016;235:34–47. doi:10.1016/j.jconrel.2016.05.044
25. Han JW, Gurunathan S, Jeong JK, et al. Oxidative stress mediated cytotoxicity of biologically synthesized silver nanoparticles in human lung epithelial adenocarcinoma cell line. *Nanoscale Res Lett*. 2014;9(1):459. doi:10.1186/1556-276X-9-459
26. Chen S, Li D, Yang F, et al. Gemcitabine-induced pancreatic cancer cell death is associated with MST1/cyclophilin D mitochondrial complexation. *Biochimie*. 2014;103:71–79. doi:10.1016/j.biochi.2014.04.004
27. Ma Y, Zhang J, Zhang Q, et al. Adenosine induces apoptosis in human liver cancer cells through ROS production and mitochondrial dysfunction. *Biochem Biophys Res Commun*. 2014;448(1):8–14. doi:10.1016/j.bbrc.2014.04.007
28. Jezek J, Cooper KF, Strich R. Reactive oxygen species and mitochondrial dynamics: the yin and yang of mitochondrial dysfunction and cancer progression. *Antioxidants*. 2018;7(1):13. doi:10.3390/antiox7010013
29. Wu H, Lin J, Liu P, et al. Reactive oxygen species acts as executor in radiation enhancement and autophagy inducing by AgNPs. *Biomaterials*. 2016;101:1–9. doi:10.1016/j.biomaterials.2016.05.031
30. Du W, Hu H, Zhang J, et al. The mechanism of MAPK signal transduction pathway involved with electroacupuncture treatment for different diseases. *Evid Based Complement Alternat Med*. 2019;2019:8138017. doi:10.1155/2019/8138017
31. Braicu C, Buse M, Busuioc C, et al. A comprehensive review on MAPK: A promising therapeutic target in cancer. *Cancer*. 2019;11(10):1618. doi:10.3390/cancers11101618

32. Dou Y, Jiang X, Xie H, He J, Xiao S. The Jun N-terminal kinases signaling pathway plays a "seesaw" role in ovarian carcinoma: a molecular aspect. *J Ovarian Res*. 2019;12(1):99. doi:10.1186/s13048-019-0573-6
33. Roy S, Roy S, Kar M, et al. p38 MAPK pathway and its interaction with TRF2 in cisplatin induced chemotherapeutic response in head and neck cancer. *Oncogenesis*. 2018;7(7):53. doi:10.1038/s41389-018-0062-6
34. Guo Y, Pan W, Liu S, et al. ERK/MAPK signalling pathway and tumorigenesis. *Exp Ther Med*. 2020;19(3):1997–2007. doi:10.3892/etm.2020.8454
35. Hammouda MB, Ford AE, Liu Y, Zhang JY. The JNK signaling pathway in inflammatory skin disorders and cancer. *Cells*. 2020;9(4):857. doi:10.3390/cells9040857
36. Grab J, Rybniker J. The expanding role of p38 mitogen-activated protein kinase in programmed host cell death. *Microbiol Insights*. 2019;12:1–3. doi:10.1177/1178636119864594
37. Zou J, Lei T, Guo P, et al. Mechanisms shaping the role of ERK1/2 in cellular senescence (Review). *Mol Med Rep*. 2019;19(2):759–770. doi:10.3892/mmr.2018.9712
38. Cao X, Wang A, Wang C, et al. Surfactin induces apoptosis in human breast cancer MCF-7 cells through a ROS/JNK-mediated mitochondrial/caspase pathway. *Chem Biol Interact*. 2010;183(3):357–362. doi:10.1016/j.cbi.2009.11.027
39. Jia Y, Wei W, Ma B, et al. Activation of p38 MAPK by reactive oxygen species is essential in a rat model of stress-induced gastric mucosal injury. *J Immunol*. 2007;179(11):7808–7819. doi:10.4049/jimmunol.179.11.7808
40. Cai Q, Teng M, Li C, Tian Y, Li H. Catalpol protects pre-myelinating oligodendrocytes against ischemia-induced oxidative injury through ERK1/2 signaling pathway. *Int J Biol Sci*. 2016;12(12):1415–1426. doi:10.7150/ijbs.16823
41. Papa S, Choy PM, Bubici C. The ERK and JNK pathways in the regulation of metabolic reprogramming. *Oncogene*. 2019;38(13):2223–2240. doi:10.1038/s41388-018-0582-8
42. Win S, Than TA, Kaplowitz N. The regulation of JNK signaling pathways in cell death through the interplay with mitochondrial SAB and upstream Post-Translational effects. *Int J Mol Sci*. 2018;19(11):3657. doi:10.3390/ijms19113657
43. Ahmad R, Vaali-Mohammed MA, Elwatidy M, et al. Induction of ROS-mediated cell death and activation of the JNK pathway by a sulfonamide derivative. *Int J Mol Med*. 2019;44(4):1552–1562. doi:10.3892/ijmm.2019.4284
44. Dhanasekaran DN, Reddy EP. JNK-signaling: a multiplexing hub in programmed cell death. *Genes Cancer*. 2017;8(9–10):682–694. doi:10.18632/genesandcancer.155